WOOD RESEARCH doi.org/10.37763/wr.1336-4561/68.3.547557
ISSN 1336-4561 e-ISSN 2729-8906
68(3): 2023 547-557 pp.

CHARACTERIZATION OF THE BURNING OF ORIENTED STRAND BOARDS EXPOSED TO FLAME

PETER RANTUCH, JOZEF MARTINKA, TOMÁŠ ŠTEFKO, IGOR WACHTER,
MÁRIA ZUZANA BEDNÁRIKOVÁ
SLOVAK UNIVERSITY OF TECHNOLOGY IN BRATISLAVA
SLOVAKIA

(RECEIVED MARCH 2022)

ABSTRACT

Since the methods based on the interaction of a relatively low intensity flame on the lignocellulose sample surface often do not allow measuring the heat release rate (HRR), a procedure using oxygen consumption calorimetry was proposed. The method was applied to OSB samples with dimensions of 320 mm x 140 mm x 25 mm placed in a vertical position. During the measurement, in addition to the HRR, the production of smoke, which was significant after stopping the burner, was also monitored. The average net value of HRR at burner outputs of 3 kW, 4 kW and 5 kW was 2.339 kW and the smoke specific extinction area was in the range of 10.88 $m^2.kg^{-1}$ and 13.19 $m^2.kg^{-1}$.

KEYWORDS: Oriented strand boards, flame, oxygen consumption calorimetry, heat release rate, smoke production.

INTRODUCTION

While characterizing wooden materials from the fire protection point of view, it is possible to encounter methods that are based on the effect of flame on their surface (Tab. 1). The advantage of such tests is their simplicity and low financial cost.

Tab. 1: An overview of publications dealing with the characterization of wood materials.

Sample	Dimensions [mm]	Sample angle [°]	Burner angle [°]	Flame height [mm]	Burner fuel	Time of applied flame [s]	Source
Spruce wood	250 x 90 x 10	90	45	20	Propane	30	(Zachar et al. 2012)
MDF board	250 x 90 x 19	90	45	20	Propane	30	(Ružinská et al.2014)
Norway spruce	200 x 100 x 10	45	90	100	-	600	(Osvaldová et al. 2016)
Betula verrucosa Ehrh.	150 × 60 x 1.5	90	90	15-25	Natural gas	120	(Bekhta et al. 2016)
Spruce wood	200 x 95 x 10	45	90	-	Propane-butane	300	(Fanfarová et al. 2016)

Thermally modified oak	200 x 100 x 20	45	90	100	Propane	600	(Gašparík et al. 2017)
Teak	200 x 100 x 20	45	90	100	Propane	600	(Čekovská et al. 2017)
Soft fibre board	250 x 90 x 40	90	45	25	Propane-butane	30	(Makovická 2017)
Teak wood	200 x 100 x 20	45	90	100	Propane	600	(Gaff et al. 2019)
Picea abies	82 x 82 x 26	0	90	50	Propane-butane	600	(Mitrenga et al. 2022)
Spruce wood	250 x 90 x 10	0; 45; 90	90	100	Propane	600	(Kmeťová et al. 2022)

The mentioned methods are mostly described by the height of the test flame and its duration, the fuel of the burner and the angle between the sample and the burner. The results are mainly expressed by the weight loss of the sample. A similar method of measurement, but on a slightly larger scale, was described by Gao et al. (2021) when monitoring the fire resistance performance of partition boards. However, the mentioned methods do not provide data on the HRR, which is currently one of the most used fire characteristics. This deficiency can be solved by oxygen consumption calorimetry.

Therefore, the aim of this article was its application to measure the behaviour of oriented strand board (OSB) exposed to flame. At the same time, the amount of released smoke was monitored optometrically, before and after the flame was applied to the sample.

MATERIAL AND METHODS

Oxygen consumption calorimetry is based on the results of (Thornton 1917), who determined that the amount of heat released during combustion strongly depends on the amount of oxygen consumed. Based on the measurements of (Huggett 1980), the HRR during a fire can be determined from the concentration of oxygen in the combustion gas products, while 13.1 kJ (± 5%) of heat is released per 1 g of oxygen consumed. This principle was also used in designing a cone calorimeter, which is currently the most widely used device for measuring HRR. It can be calculated based on the relationship (Babrauskas 1984):

$$HRR = (13.1 \times 10^3)(1.10)C\sqrt{\left(\frac{\Delta P}{T_e}\right)}\frac{(0.2095 - X_{O2})}{(1.105 - 1.5X_{O2})} \quad (1)$$

where: HRR the is heat release rate [kW], C is the orifice meter calibration constant [$m^{0.5}.kg^{0.5}.K^{0.5}$], ΔP is the orifice meter pressure differential [Pa], T_e is the temperature for the orifice meter [K], and X_{O2} is the mole fraction of oxygen in the exhaust stream [-].

The basis for determining the amount of smoke is the extinction coefficient derived from the attenuation of the light beam passing through the layer of smoke, according to (ISO 5660-1: 2015):

$$k = \frac{\ln\left(\frac{I_0}{I}\right)}{L} \quad (2)$$

where: k is the extinction coefficient [m^{-1}], I_0/I is the ratio of incident light to transmitted light [-], and L is the light path length through the smoke [m].

Based on the Eq. 2, it is possible to determine the smoke production rate (SPR) as:

$$SPR = k.\dot{V}_s \quad (3)$$

where: $\dot{V}_s$ is volume flow rate of smoke [$m^3.s^{-1}$].

The amount of released smoke can finally be expressed as a specific extinction area, σ_f [m^2.kg] (Babrauskas and Mulholland 1986):

$$\sigma_f = \frac{\sum_i k_i \dot{V}_i \Delta t_i}{m_i - m_f} \quad (4)$$

where: Σ_i is summation taken over the *i* intervals of time Δt [s], $\dot{V}$ is duct volume flow rate [$m^3.s^{-1}$], m_i is initial specimen mass [kg] and m_f is mass at the end of the test [kg].

For this study, OSB (type 3 - structural panels for use in environments with low humidity, for outdoor and indoor use) were used as samples. Their characterization is shown in Tab. 2.

Tab. 2: Characterization of OSB samples.

Density [kg.m^{-3}]		565.87 (8.54)*
Humidity [%]		6.50 (0.09)*
Proximate analysis [%w]	Volatile matter	82.04 (0.29)*
	Fixed carbon	17.51 (0.29)*
	Ash	0.45 (0.04)*
Dimensions [mm]	Height	319.8 (0.4)*
	Width	140.1 (0.1)*
	Thickness	24.8 (0.2)*

* Values in parentheses represent the respective standard deviations.

The measuring device, shown in Fig. 1, was designed based on the reduced-scale cable flammability test chamber described by (Gallo et al. 2017).

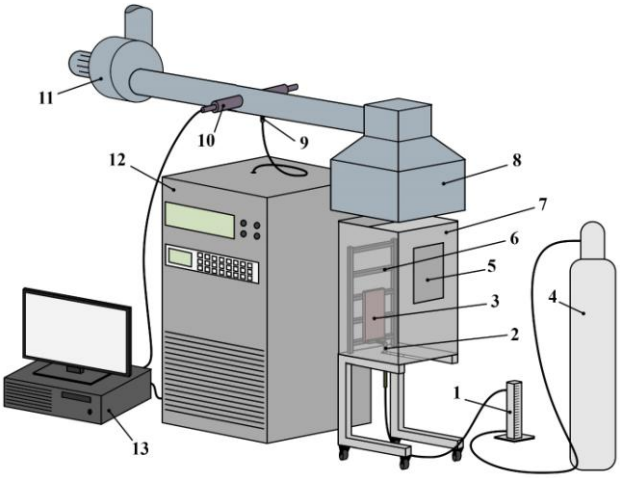

Fig. 1: Measuring device: 1) flow meter, 2) burner, 3) samples, 4) pressure vessel with fuel (methane), 5) viewing window, 6) sample holder, 7) measuring chamber, 8) hood, 9) combustion products sampling probe, 10) system for measuring the optical density of smoke, 11) adjustable fan, 12) oxygen analyzer, 13) computer.

The chamber is made of a 2 mm thick stainless steel with dimensions are 400 x 400 x 630 mm. An opening in the lower side of the chamber with an area of 20 x 160 mm is used for air supply. The combustion products are discharged through an opening in its upper part with area of 400 x 250 mm. The burner is placed at the level of the lower edge of the samples. The front side of the chamber is perforated, containing 49 holes of 1 mm diameter arranged in three rows in an area of 97 x 9 mm. For this test, methane was used as fuel, and it was regulated to the required output by the flow meter. Combustion products were extracted using a hood, placed above the test chamber. The exhaust duct contains a gas sampling probe and an optometric device for measuring the optical density of the smoke. The concentration of oxygen in the combustion products was measured by an analyzer and the obtained data were recorded on a computer in 5 s intervals.

Assuming that the combustion efficiency is close to 1 when burning combustion gases, and based on the equation of state of an ideal gas, the burner power (Q̇) in kJ can be calculated as:

$$\dot{Q} = \frac{2{,}94.\dot{V}.p.LHV_V}{273{,}15+t} \quad (5)$$

where: p is the atmospheric pressure [Pa], LHV_V is the lower heating value of the fuel measured at 25°C and 101.325 kPa [MJ.m^{-3}] and t is the temperature [°C].

Since flowmeters have a flow rate often stated in the standard litre per minute (SLPM), it is appropriate to adjust the relation (Eq.5) to the form:

$$\dot{Q} = 1{,}82.10^{-2}.LHV_V.\dot{V}_{SLPM} \quad (6)$$

where: $\dot{V}_{SLPM}$ is the fuel flow in SLPM. The values of LHV_V for selected gaseous fuels are listed in Tab. 3. In this way, the values required for this study were also determined.

Tab. 3: Characterization of selected gaseous fuels.

Fuel	**Chemical formula**	**M (g.mol^{-1})**	**LHV (MJ.m^{-3}) [a,b]**	**LHV (MJ.kg^{-1})[a]**
Hydrogen	H_2	2,02	9,9	121,2
Methane	CH_4	16,04	32,8	50,0
Ethane	C_2H_6	30,07	58,4	47,8
Propane	C_3H_8	44,10	83,6	45,4
Butane	C_4H_{10}	58,12	108	45,8
Ethylene	C_2H_4	28,05	54,1	47,2
Acetylene	C_2H_2	26,04	51,4	48,2
Propylene	C_3H_6	42,08	78,8	45,8
Natural gas	mixture of gases	mixture of gases	34,6	48,3

[a] (Bryden et al. 2022), [b] pressure of 101,325 kPa and temperature at 25°C.

Before starting the measurement, the burner was ignited out of reach of the tested sample until the fuel flow stabilized. Subsequently, it was installed under the sample at a horizontal distance of 50 mm. After 300 s from the application of the burner, the methane supply was closed, and the measurement continued for another 600 s. The ambient temperature was 21°C,

the air humidity was 39% and the atmospheric pressure was 98.9 kPa. The volume flow of the exhaust duct was set to 24 $dm^3.s^{-1}$.

Since the oxygen consumption calorimetry does not consider the type of fuel, the correction shown in Fig. 2 was made to accurately subtract the influence of the burner. The average values of the burner output were determined within periods of 180 s. The power determined by oxygen consumption calorimetry is denoted as Q_{O2} and the power calculated from the methane flow rate is denoted as Q_V.

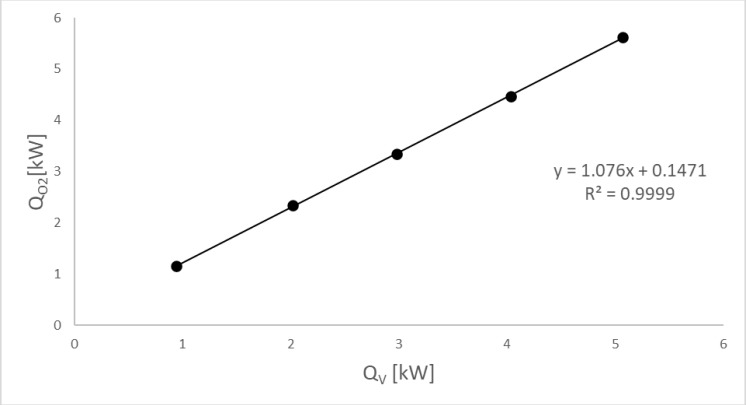

Fig. 2: Correction of the HRR determined by oxygen consumption calorimetry and calculation from methane flow.

RESULTS AND DISCUSSION

During the measurements, HRR (based on oxygen consumption calorimetry) and burner output (based on methane flow) were simultaneously monitored. An example of the measured values is shown in Fig. 3. The total HRR is pulsating, which is common in measurements based on this principle, as can be seen in the results of many studies (Martinka et al. 2014, Islam et al. 2023, Barton et al. 2022). On the contrary, the burner flow maintains a much more stable value. The graph also shows the extinguishing process, which started practically immediately after the methane supply was interrupted. The burning intensity of the OSB decreased sharply.

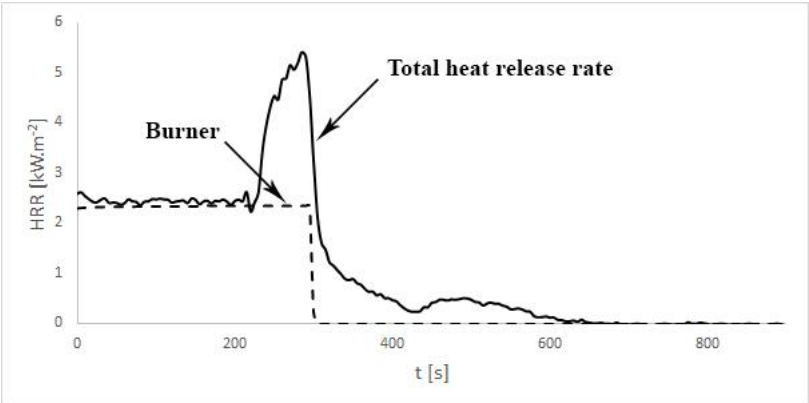

Fig. 3: Comparison of total HRR and burner output of 2 kW using OSB samples.

After turning off the methane supply, the burner output drops to zero almost immediately, but the gases accumulated in the test chamber escape more slowly. This fact leads, after the burner output is subtracted from the HRR, to a sharp peak (Fig. 4). Since this is not a short-term intensification of the burning process, this peak has been removed and replaced by a linear interpolation of the values before and after the peak. The difference between the HRR derived from the oxygen consumption calorimetry and the burner output is hereinafter referred to as the net heat release rate - ΔHRR.

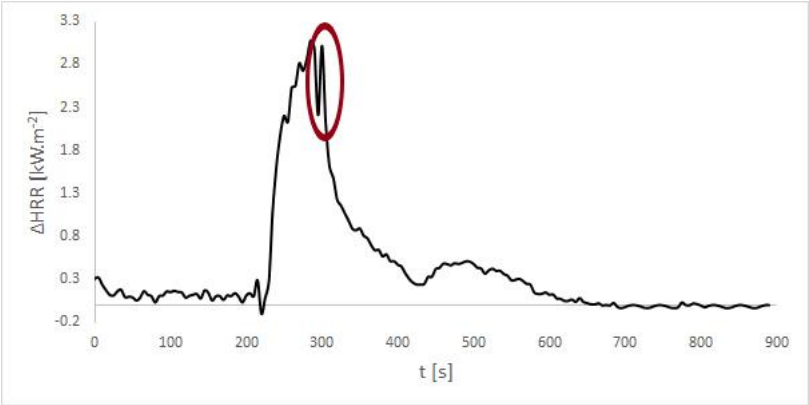

Fig. 4: Peak emerging after adjusting the total HRR by the burner output.

The area of the fire spread on the surface of the samples is illustrated after the end of the measurement (Fig. 5). At a higher burner output, flow rate of the methane reached a higher value. Visually, it was found that at an output of 2 kW, the methane flow rate was so low that the flame did not reach the sample. Therefore, ignition of sample was delayed and the burning took significantly less time than in the case of the other samples. The burned area, clearly visible from the charred layer, was also smaller. At an applied output of 3 kW, the burning of OSB still took place practically only above the plane of the burner location, but at 4 kW and 5 kW, the entire surface of the samples was affected.

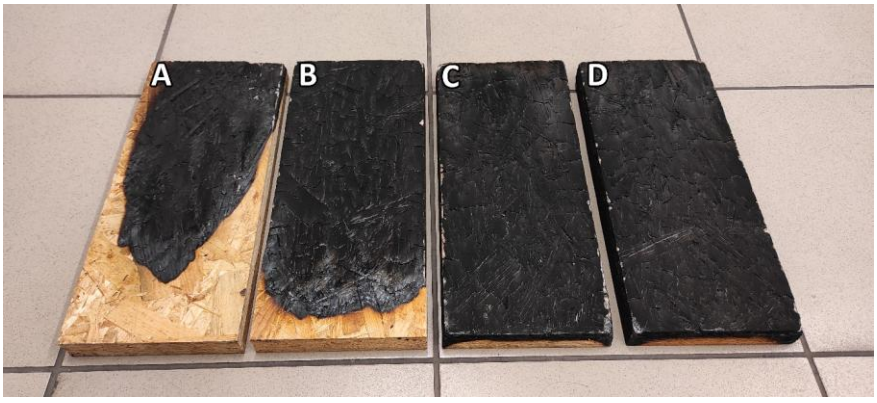

Fig. 5: Samples after the end of measurements at burner outputs of: A – 2 kW, B – 3 kW, C – 4 kW, D – 5 kW.

Net HRR and smoke production rates are shown in Fig. 6. From the graphs of all measurements is evident that turning off the methane stream (time marked by a red dashed line)

causes a sharp decrease in the ΔHRR from OSB and at the same time the SPR increases significantly. Both changes indicate the already mentioned extinguishing of the sample, and it can therefore be concluded that under the given conditions, the burning is maintained primarily by the flame of the burner. In the case of a burner output of 2 kW, delayed initiation is also evident from the course of the ΔHRR. The time to initiation can be approximately determined at 235 s, based on the HRR. Thus, the end of the methane supply followed about 65 s after the initiation of the OSB sample. In other cases, it is not possible to determine the time to initiation, as the surface of the samples was directly in the flame.

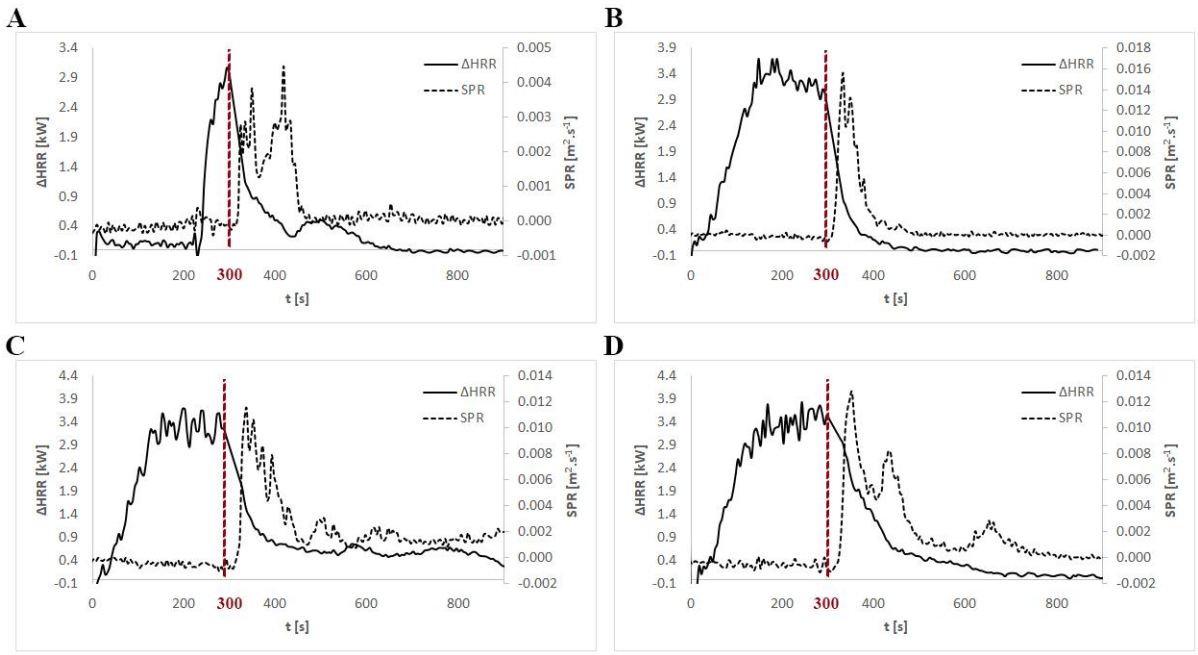

Fig. 6: Course of net HRR and smoke production rates at different burner outputs: A – 2 kW, B – 3 kW, C – 4 kW, D – 5 kW.

Determining the HRR of OSB has been the aim of many studies. According to (Ira et al. 2020, Park and Lee 2008, Hou et al. 2016) OSB behave like typical charring, thermally thick solids when measured on a cone calorimeter, as two peaks are evident in the graphs of the HRR. (Hagen et al. 2009) state that the first peak in measurements of such materials occurs due to the decomposition of the material before the formation of the char layer and the second is caused by heating the rest of the original material to the pyrolysis temperature. According to Ritchie et al. (1997), the increase in sample temperature required for the second peak is caused by the insulation placed on the opaque side of the sample. The absence of two HRR peaks in this study is probably caused by the fact that no substrate was used from the side of the OSB sample not exposed to the flame.

The results of the measurements are summarized in Tab. 4. Similar to the graphical representation of the ΔHRR over time (Fig. 6) and the photographs of the samples after the measurements (Fig. 5), the sample loaded with 2 kW burner output showed lower characteristics resulting from a lower burning intensity. Peak values of the net heat release rate (pΔHRR) and smoke production rate (pSPR) were the lowest among all samples, which can be attributed to the short burning time and small area over which it took place. Likewise, the net

total heat release (ΔTHR) and total smoke production (TSP) were the lowest, which is not surprising given the short burning time. The average ΔHRR during the operation with the burner output of 3 kW, 4 kW and 5 kW (ΔHRR_f) was similar, reaching values from 2,289 kW to 2,427 kW. Based on these data, it is possible to consider the burner output power of 2 kW under the given measurement conditions as insufficient.

The average net effective heat of combustion (ΔEHC_m) decreased with increasing burner output, reaching values from 8.69 $MJ.kg^{-1}$ to 11.90 $MJ.kg^{-1}$. Based on the smoke specific extinction area (SEA) values, it seems that the burner output did not have a significant effect on the amount of smoke released. This agrees with the above-described fact that the smoke production rate was practically zero during the operation of the burner and increased significantly only during the extinguishing of the sample.

Tab. 4: Summarization of the measurement results.

Burner output [kW]	**2**	**3**	**4**	**5**
pΔHRR [kW]	3.08	3.70	3.69	3.85
pSPR [$m^2.s^{-1}$]	0.004	0.016	0.012	0.013
ΔTHR [kJ]	357	806	1129	1123
TSP [m^2]	0.364	0.769	1.506	1.406
Δm [%]	4.85	11.08	17.93	20.61
ΔHRR_f [kW]	0.594	2.300	2.289	2.427
ΔEHC_m [$MJ.kg^{-1}$]	11.90	11.51	9.89	8.69
SEA [$m^2.g^{-1}$]	12.13	10.99	13.19	10.88

CONCLUSION

One of the drawbacks of methods for testing the fire characteristics of wood, using a small flame is that they do not provide information about the rate at which heat is released from the sample (HRR). Therefore, a measurement procedure in the testing chamber, using oxygen consumption calorimetry, was proposed. During the operation of the burner at 3 kW, 4kW and 5kW, the ΔHRR_f of the OSB samples reached 0.6 kW - 2.4 kW, depending on the burner output power. At a burner output power of 2 kW, the ΔHRR_f was significantly lower, due to the later ignition of the sample. After the end of the supply of methane, the intensity of OSB burning, and thus the ΔHRR began to decrease rapidly. At the same time, the smoke production rate (SPR) increased sharply. Total smoke production (TSP) also depended on the burner output and reached 0.4 m^2 – 1.5 m^2, while it was very similar at the output power of 4 kW and 5 kW. Converted to 1 kg of a sample, 8.69 MJ - 11.90 MJ of heat and 10880 m^2 – 13190 m^2 of smoke were released. The described measurement method can also be modified for burners with a different construction, which makes it possible to obtain a larger amount of information from relatively simple tests.

ACKNOWLEDGEMENTS

This work was supported by the VEGA agency under the contracts No. VEGA 1/0678/22. This work was supported by the Slovak Research and Development Agency under the contract No. APVV-16-0223. This work was supported by the KEGA Agency under the contract KEGA 016STU-4/2021.

REFERENCES

1. Babrauskas, V., 1984: Development of the cone calorimeter. A bench-scale heat release rate apparatus based on oxygen consumption. Fire and Materials 8: 81–95.
2. Babrauskas, V., Mulholland, G., 1988: Smoke and soot data determinations in the cone calorimeter, Mathematical Modeling of Fires, ASTM STP 983. American Society for Testing and Materials, Philadelphia, PA, pp. 83-104.
3. Barton, J., Rios, O., Runefors, M., van Hees, P., 2022: The effect of oxygen concentration on selected industrial products in the open controlled atmosphere cone calorimeter. Fire and Materials 46: 617–627.
4. Bekhta, P., Olesia, B., Sedliacik, J., Novak, I., 2016: Effect of different fire retardants on Birch plywood properties. Acta Facultatis Xylologiae 58: 59–66.
5. Bryden, K., Ragland W., K., Kong, S.-C., 2022: Combustion Engineering (3rd Ed.), 3rd Ed. ed. CRC Press. pp. 492.
6. Čekovská, H., Gaff, M., Osvaldová, L., Kačík, F., Kaplan, L., Kubs, J., 2017: *Tectona grandis* Linn. and its fire characteristics affected by the thermal modification of wood. BioResources 12: 2805–2817.
7. Fanfarová, A., Osvaldová, L., Gašpercová, S., 2016: Testing of Fire Retardants. Applied Mechanics and Materials 861: 72–79.
8. Gaff, M., Kačík, F., Gašparík, M., Todaro, L., Jones, D., Corleto, R., Makovická Osvaldová, L., Čekovská, H., 2019: The effect of synthetic and natural fire-retardants on burning and chemical characteristics of thermally modified teak (*Tectona grandis* L. f.) wood. Construction and Building Materias 200: 551–558.
9. Gallo, E., Stöcklein, W., Klack, P., Schartel, B., 2017: Assessing the reaction to fire of cables by a new bench-scale method. Fire and Materials 41: 768–778.
10. Gao, B., Wei, S., Du, W., Yang, H., Chu, Y., 2021: Experimental Study on the Fire Resistance Performance of Partition Board under the Condition of Small Fire Source. Processes: 9.10: 1818.
11. Gašparík, M., Osvaldová, L., Čekovská, H., Potůček, D., 2017: Flammability characteristics of thermally modified oak wood treated with a fire retardant. Bioresources 12: 8451–8467.
12. Hagen, M., Hereid, J., Delichatsios, M.A., Zhang, J., Bakirtzis, D., 2009. Flammability assessment of fire-retarded Nordic Spruce wood using thermogravimetric analyses and cone calorimetry. Fire Safety Journal 44: 1053–1066.

13. Hou, J., Cai, Z., Lu, K., 2016: Cone calorimeter evaluation of reinforced hybrid wood–aluminum composites. Journal of Fire Sciences 35: 118–131.
14. Huggett, C., 1980: Estimation of rate of heat release by means of oxygen consumption measurements. Fire and Materials 4: 61–65.
15. Ira, J., Hasalová, L., Šálek, V., Jahoda, M., Vystrčil, V., 2020: Thermal Analysis and Cone Calorimeter Study of Engineered Wood with an Emphasis on Fire Modelling. Fire Technology 56: 1099–1132.
16. Islam, T.M., Klinger, J.L., Toufiq Reza, M., 2023: Evaluating combustion characteristics and combustion kinetics of corn stover-derived hydrochars by cone calorimeter. Chemical Engineering Journal 452: 139419.
17. ISO, 2015. ISO 5660-1:2015 Reaction-to-Fire Tests-Heat Release, Smoke Production and Mass Loss Rate-Part 1: Heat Release Rate (Cone Calorimeter Method) and Smoke Production Rate (Dynamic Measurement).
18. Kmeťová, E., Zachar, M., Kačíková, D., 2022: The progressive test method for assessing the thermal resistance of spruce wood. Acta Facultatis Xylologiae 64: 29–36.
19. Makovická, L., 2017: Influence of the fire retardant on selected thermal insulating materials on natural base-wooden fibreboard. Pro Ligno 13.4: 101-106.
20. Martinka, J., Chrebet, T., Balog, K., 2014: An assessment of petrol fire risk by oxygen consumption calorimetry. Journal of Thermal Analysis and Calorimetry 117: 325–332.
21. Mitrenga, P., Vandlíčková, M., Konárik, M., Košútová, K., 2022: Impact of Heat Treatment of Spruce Wood on Its Fire-Technical Characteristics Based on Density and the Side Exposed to Fire. Applied Sciences 12: 6452.
22. Osvaldová, L., Gašpercová, S., Mitrenga, P., Osvald, A., 2016: The influence of density of test specimens on the quality assessment of retarding effects of fire retardants. Wood Research 61.1: 35e42.
23. Park, J.-S., Lee, J.J., 2008: Ignition and Heat Release Rate of Wood-based Materials in Cone Calorimeter Tests. Journal of the Korean Wood Science and Technology 36.2: 1-8.
24. Ritchie, S., Steckler, K., Hamins, A., Cleary, T., Yang, J., Kashiwagi, T., 1997: The Effect of Sample Size on the Heat Release Rate of Charring Materials. In: Fire Safety Science-Proceedings of the 5th International Symposium. p. 177-188.
25. Ružinská, E., Mitterova, I., Zachar, M., 2014: The Study of Selected Fire-Technical Characteristics of Special Wood Products Surface Treatment by Environmentally Problematic Coatings. Advanced Materials Research 1001: 373–378.
26. Thornton, W.M., 1917. XV. The relation of oxygen to the heat of combustion of organic compounds. The London, Edinburgh, and Dublin Philosophical Magazine and Journal of Science 33.194: 196-203.
27. Zachar, M., Mitterova, I., Xu, Q., Majlingova, A., Cong, J., Galla, Š., 2012. Determination of Fire and Burning Properties of Spruce Wood. Drvna Industrija 63.3: 217–223.

PETER RANTUCH*, JOZEF MARTINKA, TOMÁŠ ŠTEFKO, IGOR WACHTER,
MÁRIA ZUZANA BEDNÁRIKOVÁ
SLOVAK UNIVERSITY OF TECHNOLOGY IN BRATISLAVA
FACULTY OF MATERIAL SCIENCES AND TECHNOLOGY IN TRNAVA
ULICA JÁNA BOTTU 21, 91724 TRNAVA
SLOVAKIA
*Corresponding author: peter.rantuch@stuba.sk